Published in final edited form as:

J Mater Chem. 2010 March 7; 20(9): 1787–1793. doi:10.1039/b924032b.

Shape memory polymers with silicon-containing segments

Cody Alan Schoener, **Christopher Bell Weyand**, **Ranjini Murthy**, **Melissa Ann Grunlan**

Department of Biomedical Engineering, Texas A&M University, 3120 TAMU, College Station, TX, USA. mgrunlan@tamu.edu; Fax: +1 979 845 4450; Tel: +1 979 845 2406

Abstract

Thermoresponsive shape memory polymers are stimuli-responsive materials whose shape is modulated by heat. They have been investigated as smart materials in a variety of biomedical, industrial and aerospace applications. The vast majority of shape memory polymers have been limited to those prepared from organic polymers. In this present work, shape memory polymers comprised of inorganic silicon-containing polymer segments (polydimethylsiloxane, PDMS) and organic poly(ε-caprolactone) (PCL) segments were developed. Because of its low T_g, PDMS served as a highly effective soft segment. The photochemical cure of diacrylated PCL$_n$-*block*-PDMS$_{37}$-*block*-PCL$_n$ macromers with tailored PCL segment lengths produced networks with excellent mechanical properties, shape fixity, and shape recovery.

Introduction

Shape memory polymers (SMPs) are stimuli-responsive materials which change their shape upon application of an external stimulus such as heat.[1,2] Compared to shape memory alloys (SMAs) and shape memory ceramics, SMPs are lightweight, readily fabricated, exhibit greater elastic deformation, and optionally are biodegradable.[3] These properties have prompted their investigation into a variety of biomedical applications.[1–7] New thermoresponsive SMPs with sharp and tunable transition temperatures (T_{trans}) to actuate shape change, high strain recovery and fixity, high moduli to withstand tensile and compressive forces, and high elasticity should lead to improved and new devices in medical as well as other fields. In general, hybrid materials comprised of inorganic (*e.g.* silicon-based) and organic polymer components have attracted interest to yield properties superior to that of parent materials.[8–12] However, SMPs formed from silicon (Si)-containing inorganic and organic polymer components have been limited to a single report.[13]

The shape memory effect of SMPs is attributed to switching segments and net points which work cooperatively.[1] The net points determine the permanent shape and may be either chemical or physical crosslinks formed *via* covalent bonds or molecular interactions, respectively. The switching segment exhibits a thermal transition temperature (T_{trans}) which corresponds to either the glass transition (T_g) or melting transition (T_m). Thus, a temporary shape formed by the application of stress at $T > T_{trans}$ is fixed by cooling the deformed SMP at $T < T_{trans}$ and the permanent shape subsequently recovered by reheating to $T > T_{trans}$. The ability of an SMP to maintain its temporary shape at $T < T_{trans}$ and to recover its permanent shape at $T > T_{trans}$ is referred to as strain fixity and strain recovery, respectively. SMPs based on both physically and chemically crosslinked poly-(ε-caprolactone) (PCL; T_g = −60 °C)

have received much attention due to PCLs biodegradability and elasticity.[14,15] PCL is an effective crystalline switching segment in which the T_m serves as the T_{trans} of the network. The T_m of PCL is well-defined and increases with M_n (43–60 °C) which is in the range useful for deployment in *vivo*.[16] To manipulate the thermomechanical properties of PCL-based SMPs, other organic polymeric components have been introduced, including: polyurethanes,[17–19] poly(L-lactide),[20–24] poly(glycolide),[25] poly(ethylene glycol),[26] poly(*p*-dioxanone)[27] and poly(*n*-butyl acrylate).[28]

The lack of PCL-based SMPs which incorporate an inorganic polymer component prompted us to explore the introduction of polydimethylsiloxane (PDMS), a polymer with an inorganic backbone. PDMS has many interesting properties, including: good biocompatibility, thermal and oxidative stability, and gas permeability.[29,30] In particular, its exceptionally low T_g (−125 °C) makes PDMS a very effective "soft segment" which should enhance the deformability (*i.e.* % strain at break) of the SMPs. SMPs based on a combination of PCL and polysiloxanes have been limited to those prepared *via* the radiation crosslinking of physical blends of PCL (M_w = 50k g mol^{-1}; 80–95 wt%) with polymethylvinylsiloxane (PMVS; M_n ≈ 60 kg mol^{-1}; 5–20 wt%).[13] However, blends could only be prepared with less than 20 wt% of PMVS due to blend instability. In addition, networks with less than 50% sol (i.e. uncrosslinked material) were not achieved and radiation-induced chain scission of PCL led to diminished strength.

In the present work, we report inorganic–organic SMPs formed via the photochemical cure of a series of photosensitive triblock macromers consisting of a central inorganic PDMS segment and terminal organic PCL segments of varying lengths (Fig. 1). Six compositionally unique photosensitive macromers were prepared with the general formula: AcO-PCL$_n$-block-PDMS$_{37}$-*block*-PCL$_n$-OAc (n = 5, 10, 20, 30, 40 and 50). Following the photochemical cure of each macromer, the thermal, mechanical, and shape memory properties of the resulting networks were tested and related to composition.

Experimental

Materials

ε-Caprolactone, triethylamine (Et_3N), acryloyl chloride, stannous 2-ethylhexanoate, 2,2-dimethoxy-2-phenylacetophenone (DMAP), 1-vinyl-2-pyrrolidinone (NVP), 4-(dimethylamino)-pyridine (DMP), K_2CO_3, poly(dimethylsiloxane)-bis(3-aminopropyl) terminated (NH_2 -PDMS$_{37}$-NH_2; M_n = 3000 g mol^{-1} by ^{1}H NMR end-group analysis) and solvents were obtained from Aldrich. Reagent-grade CH_2Cl_2, $CHCl_3$, and NMR-grade $CDCl_3$ were dried over 4 Å molecular sieves.

Macromer synthesis and characterization

The HO-PCL$_n$-*block*-PDMS$_{37}$-*block*-PCL$_n$–OH macromers (n = 5, 10, 20, 30, 40 and 50) (**a**) were prepared by ring-opening polymerization of ε-caprolactone in the presence of bis-(3-aminopropyl) terminated PDMS (NH_2-PDMS$_{37}$-NH_2) and a tin catalyst (Fig. 1).[31] The segment length of the PCL blocks was controlled by the ratio of 3-caprolactone to NH_2-PDMS$_{37}$-NH_2. The terminal hydroxyl groups were subsequently converted to photosensitive

acrylate (OAc) groups by reaction with acryloyl chloride to yield AcO-PCL$_n$-*block*-PDMS$_{37}$-*block*-PCL$_n$-OAc macromers (**b**). The number average molecular weight (M_n) as well as PDMS and PCL segment lengths were determined by ^{1}H NMR.

Synthesis of a-p1.—NH_2-$PDMS_{37}$-NH_2 (20.0 g, 6.69 mmol), ε-caprolactone (7.17 g, 62.89 mmol), and stannous 2-ethylhexanoate (0.043 g, 0.11 mmol) were combined in a 250 mL round-bottomed (rb) flask equipped with rubber septum and magnetic Teflon stir bar. The reaction was stirred for 24 h at 145 °C under N_2. After cooling to room temperature (RT), the crude product was dissolved in a minimal amount of $CHCl_3$ and precipitated twice in an excess of cold (~10 °C) methanol. The isolated product was dried under vacuum at 45 °C for 20 h. In this way, **a-p1** (19.33 g, 71% yield; M_n = 4126 g mol^{-1}) was obtained as a viscous, yellow liquid. M_n and PDMS : PCL ratio were determined by ^{1}H NMR spectroscopy. δ_H (300 MHz, $CDCl_3$): 0.11–0.40 (br m, 240H, $SiCH_3$), 0.49 (m, 4H, −$SiCH_2CH_2CH_2$−), 1.35 (m, 20H, −$CH_2CH_2CH_2CH_2CH_2$–OH),1.58 (m, 40H, −$CH_2CH_2CH_2CH_2CH_2$–OH), 2.11 (m, 4H, −$SiCH_2CH_2CH_2$-), 2.27 (m, 20H, −$CH_2CH_2CH_2CH_2CH_2$–OH),3.18 (m, 4H, −$SiCH_2CH_2CH_2$−), 3.60 (m, 4H, NH), 4.02 (m, 20H, −$CH_2CH_2CH_2CH_2CH_2OH$).

Synthesis of a-p2.—NH_2−$PDMS_{37}$–NH_2 (15.0 g, 5.0 mmol), ε-caprolactone (10.76 g, 94.4 mmol), and stannous 2-ethylhexanoate (0.043 g, 0.11 mmol) were reacted as above. In this way, **a-p2** (24.88 g, 97% yield; M_n = 5266 g mol $^{-1}$) was obtained as a viscous, yellow liquid. δ_H (300 MHz, $CDCl_3$): 0.35–0.11 (br m, 240H, $SiCH_3$), 0.50 (m, 4H, −$SiCH_2CH_2CH_2$−),1.39 (m, 40H, −$CH_2CH_2CH_2CH_2CH_2OH$), 1.61 (m, 80H, −$CH_2CH_2CH_2CH_2CH_2OH$), 2.11 (m, 4H, −$SiCH_2CH_2CH_2$−), 2.29 (m, 40H, −$CH_2CH_2CH_2CH_2CH_2OH$), 3.20 (m, 4H, −$SiCH_2CH_2CH_2$−), 3.63 (m, 2H, NH), 4.05 (m, 40H, −$CH_2CH_2CH_2CH_2CH_2OH$).

Synthesis of a-p3.—NH_2-$PDMS_{37}$–NH_2 (7.57 g, 2.52 mmol), ε-caprolactone (10.85 g, 95.06 mmol), and stannous 2-ethylhexanoate (0.043 g, 0.11 mmol) were reacted as above. In this way, **a-p3** (14.37 g, 78% yield; M_n = 7546 g mol^{-1}) was obtained as a yellow wax. δ_H (300 MHz, $CDCl_3$): 0.03–0.11 (br m, 240H, $SiCH_3$), 0.50 (m, 4H, -$SiCH_2CH_2CH_2$-), 1.39 (m, 80H, -$CH_2CH_2CH_2CH_2CH_2OH$), 1.58 (m, 160H, -$CH_2CH_2CH_2CH_2CH_2OH$), 2.11 (m, 4H, -$SiCH_2CH_2CH_2$-), 2.29 (m, 80H, -$CH_2CH_2CH_2$-CH_2CH_2OH), 3.22 (m, 4H, -$SiCH_2CH_2CH_2$-), 3.61 (m, 2H, NH), 4.04 (m, 80H, -$CH_2CH_2CH_2CH_2CH_2OH$).

Synthesis of a-smp1.—NH_2-$PDMS_{37}$–NH_2 (5.0 g, 1.67 mmol), ε-caprolactone (10.78 g, 100.21 mmol), and stannous 2-ethylhexanoate (0.043 g, 0.11 mmol) were reacted as above. In this way, **a-smp1** (10.36 g, 66% yield; M_n = 9826 g mol $^{-1}$) was obtained as a yellow wax. δ_H (300 MHz, $CDCl_3$): 0.03–0.12 (br m, 240H, $SiCH_3$), 0.51 (m, 4H, -$SiCH_2CH_2CH_2$-), 1.41 (m, 120H, -$CH_2CH_2CH_2CH_2CH_2OH$), 1.63 (m, 240H, -$CH_2CH_2CH_2CH_2CH_2OH$), 2.11 (m, 4H, -$SiCH_2CH_2CH_2$-), 2.27 (m, 120H, -$CH_2CH_2CH_2CH_2CH_2OH$), 3.21 (m, 4H, -$SiCH_2CH_2CH_2$-), 3.64 (m, 2H, NH), 4.05 (m, 120H, -$CH_2CH_2CH_2CH_2CH_2OH$).

Synthesis of a-smp2.—NH_2-$PDMS_{37}$–NH_2 (6.71 g, 2.24 mmol), ε-caprolactone (19.26 g, 169.0 mmol), and stannous 2-ethylhexanoate (0.043 g, 0.11 mmol) were reacted as above. In this way, **a-smp2** (20.25 g, 77% yield; M_n = 12 106 g mol $^{-1}$) was obtained as a yellow wax. δ_H (300 MHz, $CDCl_3$): 0.03–0.13 (br m, 240H, $SiCH_3$), 0.52 (m, 4H, -$SiCH_2CH_2CH_2$-),1.38 (m, 160H, -$CH_2CH_2CH_2CH_2CH_2OH$), 1.60 (m, 320H, -$CH_2CH_2CH_2CH_2CH_2OH$), 2.16 (m, 4H, -$SiCH_2CH_2CH_2NH$-), 2.27 (m, 160H, -$CH_2CH_2CH_2CH_2CH_2OH$), 3.20 (m, 4H, -$SiCH_2CH_2CH_2$-), 3.63 (m, 2H, NH), 4.05 (m, 160H, -$CH_2CH_2CH_2CH_2CH_2OH$).

Synthesis of a-smp3.—NH_2-$PDMS_{37}$–NH_2 (6.0 g, 2.0 mmol), ε-caprolactone (22.26 g, 195.3 mmol), and stannous 2-ethylhexanoate (0.043 g, 0.11 mmol) were reacted as above. In this way, **a-smp3** (23.44 g, 83% yield; M_n = 14 386 g mol $^{-1}$) was obtained as a yellow wax. δ_H (300 MHz, $CDCl_3$): 0.12–0.15 (br m, 240H, $SiCH_3$), 0.50 (m, 4H, -$SiCH_2CH_2CH_2$-), 1.39 (m, 200H, -$CH_2CH_2CH_2CH_2CH_2OH$), 1.64 (m, 400H, -$CH_2CH_2CH_2CH_2CH_2OH$), 2.14 (m, 4H, -$SiCH_2CH_2CH_2NH$-), 2.31 (m, 200H, -$CH_2CH_2CH_2$-CH_2CH_2OH), 3.19 (m, 4H, –Si-$CH_2CH_2CH_2$-), 3.65 (m, 2H, NH), 4.05 (m, 200H, -$CH_2CH_2CH_2$-CH_2CH_2OH).

Synthesis of b-p1. a-p1—(19.33 g, 4.68 mmol), DMP (0.0023 g,0.02 mmol), Et_3N (0.909 g, 8.99 mmol), acryloyl chloride (1.62 g,17.98 mmol) and dry CH_2Cl_2 (140 mL) were combined in a 250 mL rb flask equipped with a Teflon stir bar, rubber septum, and purged with N_2. Et_3N was slowly added to the solution followed by the dropwise addition of acryloyl chloride. After 30 min, the mixture was refluxed at 50 °C for 20 h. The solvent was removed under reduced pressure, the crude product dissolved in ethyl acetate and filtered to remove triethylamine hydrochloride salts. After removing solvent under reduced pressure, the isolated product was dissolved in CH_2Cl_2 (130 mL), and washed with 2 M K_2CO_3 (12 mL). After allowing the layers to separate overnight, the organic layer was isolated, dried with $MgSO_4$, gravity filtered, and volatiles removed under reduced pressure. In this way, b-p1 (15.29 g, 73% yield; M_n = 4324 g mol $^{-1}$) was obtained as a tacky, yellowish solid. ^{1}H NMR spectroscopy confirmed diacrylation and maintenance of PDMS : PCL ratio and M_n. δ_H (300 MHz, $CDCl_3$): 0.03–0.11 (br m, 240H, $SiCH_3$), 0.49 (m, 4H, -$SiCH_2CH_2CH_2$-), 1.39 (m, 20H, -$CH_2CH_2CH_2CH_2CH_2O$-), 1.58 (m, 40H, -$CH_2CH_2CH_2CH_2CH_2O$-), 2.11 (m, 4H, -$SiCH_2CH_2CH_2$-), 2.27 (m, 20H, -$CH_2CH_2CH_2CH_2CH_2O$-), 3.19 (m, 4H, -$SiCH_2CH_2CH_2$-), 3.61 (m, 2H, NH), 4.02 (m, 12H, -$CH_2CH_2CH_2CH_2CH_2O$-), 5.82 (dd, 2H, J = 10.5 and 1.5 Hz, -CH]CH_2), 6.11 (dd, 2H, J = 17.4 and 10.5 Hz, -CH == CH_2),6.40 (dd, 2H, J = 17.4 and 1.8 Hz, -CH == CH_2).

Synthesis of b-p2. a-p2—(24.88 g, 4.73 mmol), DMP (0.0023 g,0.02 mmol), Et_3N (0.985 g, 9.74 mmol), acryloyl chloride(1.76 g, 19.44 mmol) were reacted as above. In this way, **b-p2**(17.40 g, 66% yield; M_n = 5374 g mol^{-1}) was obtained as a tacky, yellow solid. δ_H (300 MHz, $CDCl_3$): 0.05–0.11 (br m, 240H, $SiCH_3$), 0.51 (m, 4H, -$SiCH_2CH_2CH_2NH$-), 1.39 (m, 40H, -$CH_2CH_2CH_2CH_2CH_2O$-), 1.60 (m, 80H, -$CH_2CH_2CH_2CH_2CH_2O$-), 2.12 (m, 4H, -$SiCH_2CH_2CH_2NH$-), 2.27 (m, 40H, -$CH_2CH_2CH_2CH_2CH_2$-), 3.22 (m, 4H, -$SiCH_2CH_2CH_2NH$-), 3.61 (m, 2H, NH), 4.10 (m, 40H, -$CH_2CH_2CH_2CH_2CH_2O$-), 5.82 (dd, 2H, J = 10.5 and 1.8 Hz, -CH]CH_2), 6.11 (dd, 2H, J = 17.4 and 10.5 Hz, -CH == CH_2),6.40 (dd, 2H, J = 17.3 and 1.7 Hz, -CH == CH_2).

Synthesis of b-p3. a-p3—(14.37 g, 1.90 mmol), DMP (0.0023 g,0.02 mmol), Et_3N (0.372 g, 3.68 mmol), acryloyl chloride (0.664 g, 7.37 mmol) were reacted as above. In this way, **b-p3** (5.02 g, 33% yield; M_n = 7654 g mol^{-1}) was obtained as a tacky, yellow solid. δ_H (300 MHz, $CDCl_3$): 0.05–0.11 (br m, 240H, $SiCH_3$), 0.50 (m, 4H, -$SiCH_2CH_2CH_2NH$-), 1.39 (m, 80H, -$CH_2CH_2CH_2CH_2CH_2O$-), 1.60 (m, 160H, -$CH_2CH_2CH_2CH_2CH_2O$-), 2.11 (m, 4H, -$SiCH_2CH_2CH_2NH$-), 2.31 (m, 80H, -$CH_2CH_2CH_2$-CH_2CH_2O-), 3.22 (m, 4H, -$SiCH_2CH_2CH_2NH$-), 3.70 (m, 2H, NH), 4.05 (m, 80H, -$CH_2CH_2CH_2CH_2CH_2O$-), 5.82 (dd, 2H, J = 10.5 and 1.5 Hz, -CH == CH_2), 6.11 (dd, 2H, J = 17.4 and 10.5 Hz, -CH == CH_2), 6.40 (dd, 2H, J = 17.4 and 1.5 Hz, -CH == CH_2).

Synthesis of b-smp1. a-smp1—(10.36 g, 1.05 mmol), DMP(0.0023 g, 0.02 mmol), Et_3N (0.210 g, 2.07 mmol), acryloyl chloride (0.374 g, 4.14 mmol) were reacted as above. In this way, **b-smp1** (4.73 g, 46% yield, M_n = 9934 g mol^{-1}-CH]CH_2), was obtained as a waxy, yellow solid. δ_H (300 MHz, $CDCl_3$): 0.008–0.14 (br m, 240H, SiCH3), 0.51 (m, 4H, -$SiCH_2CH_2CH_2NH$-),1.39 (m, 120H, -$CH_2CH_2CH_2CH_2CH_2O$-), 1.61 (m, 240H, -$CH_2CH_2CH_2CH_2CH_2O$), 2.11 (m, 4H, -$SiCH_2CH_2CH_2NH$-), 2.29 (m, 120H, -$CH_2CH_2CH_2$-CH_2CH_2O-), 3.21 (m, 4H,-$SiCH_2CH_2CH_2NH$-), 3.64 (m, 2H, NH), 4.02 (m, 120H,-$CH_2CH_2CH_2CH_2CH_2O$-), 5.82 (dd, 2H, J = 10.2 and 1.5 Hz -CH == CH_2),6.11 (dd, 2H, J = 17.4 and 10.5 Hz, -CH == CH_2),6.40 (dd, 2H, J = 17.7 and 1.8 Hz, -CH == CH_2).

Synthesis of b-smp2. a-smp2—(20.25 g, 1.67 mmol), DMP(0.0023 g, 0.02 mmol), Et_3N (0.343 g, 3.39 mmol), acryloyl chloride (0.612 g, 6.78 mmol) were reacted as above. In this way, **b-smp2** (11.44 g, 55% yield; M_n = 12 214 g mol^{-1}) was obtained as a waxy, yellow solid. δ_H (300 MHz, $CDCl_3$): 0.046–0.10 (br m, 240H, $SiCH_3$), 0.53 (m, 4H, -$SiCH_2CH_2CH_2NH$-), 1.39 (m, 160H, -$CH_2CH_2CH_2CH_2CH_2O$-), 1.63 (m, 320H, -$CH_2CH_2CH_2CH_2CH_2O$-), 2.11 (m, 4H, -$SiCH_2CH_2CH_2NH$-), 2.31 (m, 160H, -$CH_2CH_2CH_2$-CH_2CH_2O-), 3.22 (m, 4H, -$SiCH_2CH_2CH_2NH$-), 3.64 (m, 2H, NH), 4.06 (m, 160H, -$CH_2CH_2CH_2CH_2CH_2O$-), 5.83 (dd, 2H, J = 10.4 and 1.5 Hz, -CH == CH_2), 6.11 (dd, 2H, J = 17.4 and 10.5 Hz, -CH == CH_2), 6.40 (dd, 2H, J = 17.4 and 1.8 Hz, -CH == CH_2).

Synthesis of b-smp3. a-smp3—(23.44 g, 1.62 mmol), DMP(0.0023 g, 0.02 mmol), Et_3N (0.343 g, 3.39 mmol), acryloyl chloride (0.612 g, 6.78 mmol) were reacted as above. In this way, **b-smp3** (6.7 g, 28% yield; M_n = 14 494 g mol^{-1}) was obtained as a waxy, yellow solid. δ_H (300 MHz, $CDCl_3$): 0.06–0.11 (br m, 240H, $SiCH_3$), 0.55 (m, 4H, -$SiCH_2CH_2CH_2NH$-), 1.40 (m, 200H, -$CH_2CH_2CH_2CH_2CH_2O$-), 1.65 (m, 400H, -$CH_2CH_2CH_2CH_2CH_2O$-), 2.20 (m, 4H, -$SiCH_2CH_2CH_2NH$-), 2.32 (m, 200H, -$CH_2CH_2CH_2$-CH_2CH_2O-), 3.22 (m, 4H, -$SiCH_2CH_2CH_2NH$-), 3.64 (m, 2H, NH), 4.06 (m, 200H, -$CH_2CH_2CH_2CH_2CH_2O$-), 5.83 (dd, 2H, J = 10.4 and 1.5 Hz, -CH == CH_2), 6.11 (dd, 2H, J = 17.4 and 10.5 Hz, -CH == CH_2),6.41 (dd, 2H, J = 17.4 and 1.8 Hz, -CH === CH_2).

Photocrosslinking

To form crosslinked networks, each acrylated macromer (**b-p1–3** and **b-smp1–3**) was dissolved in CH_2Cl_2 at 25 wt%. To each 1 mL of the resulting precursor solution was added

150 μL of photocatalyst solution [10 wt% solution of 2,2-dimethoxy-2-phenylacetophenone (DMAP) in 1-vinyl-2-pyrrolidinone (NVP)]. The precursor solution was pipetted into a circular silicone mold (45 mm × 2 mm; McMaster-Carr) sandwiched between glass slides and exposed to UV light (UV-Transilluminator, 6 mW cm^{-2}, 365 nm) for 3 min. The resulting solvent-swollen disc was removed from the mold, air dried (RT, 12 h), and dried *in vacuo* (36 inHg, 80 °C, 4 h) to remove solvent. Uncrosslinked material was removed by soaking the disc in ethanol (3 h), air drying overnight, and drying *in vacuo* (36 inHg, 80 °C, 4 h).

Thermal characterization

Differential scanning calorimetry (DSC, TA Instruments Q100) of network specimens in hermetic pans was ran from −150 to 95 °C at a heating rate of 5 °C min^{-1} for two cycles. From the endothermic melting peak of the second cycle, temperature of crystalline melt (T_m), enthalpy change (ΔH_m) and percent crystallinity (% χ_c) were measured. The percent crystallinity (% χ_c) was calculated as follows:

$$\%\chi_c = \frac{\Delta H_m}{\Delta H_m^0} \times 100 \quad (1)$$

where ΔH_m was calculated by area of the melting peak and ΔH°_m is the enthalpy of fusion of 100% crystalline PCL (139.5 J g^{-1}).[32]

Mechanical characterization

Tensile properties of networks were evaluated at room temperature with a tensile tester (Instron 3340) by subjecting rectangular strips (~ 20 mm × ~ 3.3 mm × ~ 1.1 mm) to a constant strain rate (50 mm min^{-1}) in tension until they broke.[33]From the resulting stress–strain curves, modulus (E), tensile strength (TS), and percent strain at break (% ε) were determined.

Shape memory behavior

Shape memory properties of networks were measured *via* strain-controlled cyclic thermal–mechanical tensile tests over four cycles (N). Rectangular specimens (~ 7 mm × ~ 3 mm × ~ 1.1 mm) were subjected to the following sequence: (1) after equilibrating at 80 °C (T_{high}) for 5 min, elongate to a maximum strain(ε_m = 75%) at a rate of 50% strain min^{-1} (or 3.1 mm min^{-1}), (2) hold at ε_m for 5 min and then cool to 25 °C (T_{low}) to fix the temporary shape, (3) remove load and immediately measure ε_u and (4) reheat the sample to 80 °C (T_{high}) to recover to the permanent shape and measure ε_p, and then begin the second cycle. The shape memory effect was quantified by strain fixity (R_f), strain recovery (R_r), and total strain recovery ($R_{r,tot}$).[3] Strain fixity (R_f) quantifies the ability of the material to maintain a mechanical deformation (ε_m) after cooling resulting in a temporary deformation (ε_u):

$$R_f(N) = \frac{\varepsilon_u(N)}{\varepsilon_m} \quad (2)$$

For each cycle (N), strain recovery rate (R_r) quantifies the ability of a material to return to its permanent shape (ε_p) after application of mechanical deformation (ε_m):

$$R_r(N) = \frac{\varepsilon_m - \varepsilon_p(N)}{\varepsilon_m - \varepsilon_p(N-1)} \quad (3)$$

where $\varepsilon_p(N-1)$ and $\varepsilon_p(N)$ are the strains of the sample in two

successively passed cycles in the stress-free state. Total strain recovery rate ($R_{r,tot}$) is defined as the total recovered strain for each independent cycle ($\varepsilon_p(N)$) as compared to the original strain deformation (ε_m):

$$R_{r,tot}(N) = \frac{\varepsilon_m - \varepsilon_p(N)}{\varepsilon_m} \quad (4)$$

Results and discussion

Introduction of PDMS as a soft segment to PCL-based SMPs was accomplished with series of photosensitive AcO-PCL$_n$-*block*-PDMS$_{37}$-*block*-PCL$_n$-OAc macromers (**b**). These were prepared with a synthetic strategy which permitted the systematic control of PCL segment length and hence macromer PDMS : PCL ratio, M_n and crosslink density of the resulting networks (Fig. 1).Networks (**P1–3** and **SMP1–3**) were formed *via* the rapid photochemical crosslinking of a precursor solution consisting of a designated macromer (**b**) dissolved in CH_2Cl_2 at a concentration of 25 wt%. As a photo-crosslinked system, crosslinking was rapid and permitted spatial and temporal control.[35] Uncrosslinked macromer (*i.e.* sol) was removed from crosslinked networks *via* soaking samples in ethanol. The % sol extracted was less than 10 wt% in all cases and did not significantly increase with further soaking. Network compositions are summarized in Table 1.

Networks **P1** and **P2** exhibited no melting transition whereas **P3** and **SMP1–3** did (Table 1). The PCL segments of **P1** (n = 5) and **P2** (n = 10) were apparently too short to permit the devel-opment of crystallites. **P3** (n = 20) exhibited a low T_m (34 °C) and its ΔH_m (23 J g^{-1}) and % crystallinity (17%) values were somewhat lower compared to **SMP1–3**. With increasing PCL segment lengths, **SMP1** (n = 30), **SMP2** (n = 40), and **SMP3** (n = 50) exhibited similar T_m values (50–52 °C) to each other and ΔH_m (33–42 J g^{-1}) and crystallinity (24–30%) increased somewhat. The increased level of network crystallinity with longer PCL segment length is visually apparent in the higher opacity of specimens (Fig. 1).

The mechanical properties of polymer networks were characterized by tensile tests (Table 1). For covalently crosslinked networks, an increase in molecular weight between crosslinks gives rise to a lower crosslink density which typically results in a decrease in E and TS but an increase in % ε.[36] Indeed for these networks, values of % ε dramatically increased from 156% (**P1**) to 1197% (**SMP3**) as the PCL segment length (n) and total macromer M_n increased which produced a lower crosslink density. However, an unusual simultaneous increase in E and TS was observed as % ε increased. E increased from 0.7 MPa (**P1**) to60.5 MPa (**SMP3**) and TS increased from 0.3 MPa (**P1**) to 15.9 MPa (**SMP3**). These increases may be attributed to the increased formation of PCL crystalline domains as PCL segment length increases which act as physical crosslinks to reinforce the network even as the crosslink density decreases. Other approaches to extend the mechanical properties of PCL-based SMPs have been reported but do not result in concomitant, systematic increases in E, TS, and % ε. Furthermore, high values of % ε achieved are also notable compared to many other PCL-based SMPs. For example, for the photochemical cure of oligo(ε-caprolactone)dimethacrylates (M_n = 1.5–10k g mol^{-1}),increased macromer M_n produced networks whose % ε increased (16–296%) but E (71 to 2.4 MPa) and TS (16.2 to 0.4 MPa) simultaneously decreased.[37] PCL-based shape memory “AB polymer networks” have also been formed by incorporation of a second segment (i.e. comonomer). For instance, poly(L-lactide) (PLLA, T_m = 175–178 °C, T_g = 65 °C) was introduced as a hard segment *via* the photocuring of multiblock copolymers consisting of PLLA, PCL, and photosensitive chain extender segments.[24] For networks lacking high sol contents (*i.e.* <20% sol), increased PLLA content generally produced networks with higher E (160–720 MPa) and TS (14–24 MPa) values but lower % ε (430 to 260%). Thermoplastic AB networks have been formed by the introduction of poly(*p*-dioxanone) (PD; T_m = 110 °C, T_g = 10 °C) as a crystallizable hard segment (*i.e.* net=points) by using multiblock copolymers comprised of PD, PCL, and a coupling agent.[27] Increased PD content (9–83 wt%) generally produced networks with increasing E (34–90 MPa) and TS (13–25 MPa) but with concomitant decrease in % ε (1100 to 650%).

Because of the low T_g of poly(*n*-butyl acrylate) (T_g = 55 °C), AB networks containing soft segments were prepared by cross-linking *n*-butyl acrylate with oligo(ε-caprolactone)dimethacrylates (PCL–DA; M_n = 2k or 10k g mol^{-1}).[28] As *n*-butyl acrylate content increased (20–71 wt% for 10k g mol^{-1} PCL–DA), crosslink density decreased and networks generally exhibited an increase in % ε (290–555%) but with a simultaneous decrease in E (58 MPa to ~ 7.8 MPa) and TS (14.6 to 4.3 MPa) values. Because of their lower T_g*s*, polysiloxanes are expected to be particularly good soft segments for PCL-based SMPs. For radiation cured (100 kGy) PCL–PMVS blends, SMP networks had extremely high sol content (>70 wt%) and as PMVS content increased (~ 2 to 13 wt%), these networks exhibited a decrease in TS (21.1 to12.7 MPa) and nearly unchanged % ε (227–267%) values.[13] Thus, in this study, the PDMS segment is a particularly effective softening segment for PCL networks due to its extremely low T_g (−125 °C) which gives rise to exceptionally high % ε values. In addition, the PDMS soft segments permit the crystallization of PCL segments of sufficient length such that E and TS are also enhanced.

Shape memory properties of networks were measured *via* strain-controlled cyclic thermal–mechanical tensile tests over four cycles (N). R_f, R_r, and $R_{r,tot}$ for **SMP1–3** are shown as a function of cycle number in Table 2. **P1–3** exhibited no shape memory effect because of the lack of switching segments since the PCL segments were of insufficient length to sufficiently crystallize as confirmed by DSC. At longer PCL segment lengths (n = 30–50), the PCL segments exhibited substantial crystallization which led to a shape memory effect for **SMP1–3**. Ideally, R_f, R_r, and $R_{r,tot}$ should be 100%. For **SMP1–3**, R_f of **SMP2** and **SMP3** were essentially 100% after each cycle indicating a perfect ability to fix the temporary deformed shape. For **SMP1**, R_f was just slightly lower (~ 98%). Thus, as crosslink density decreased (**SMP1 > SMP2 > SMP3**), the ability of the PCL switching segments to maintain the deformed shape was not diminished. Shape recovery (R_r and $R_{r,tot}$) of **SMP1–3** approached 100% and was not significantly different from each other. Thus, the shape recovery is not affected by changes in crosslink density and the PCL blocks were also able to effectively "switch" to a mobile state at $T > T_{trans}$. A decrease in shape recovery was observed with each successive cycle with the largest decrease occurring between cycles 1 and 2 and becoming smaller with subsequent cycles. This trend is commonly exhibited by SMPs and the larger recovery decrease between cycle 1 and 2 attributed to extensive chain alignment of original cast films.[22,38] A photosequence demonstrating the macroscopic shape memory effect of **SMP1** is shown in Fig. 2.

Conclusions

To summarize, shape memory polymers (SMPs) comprised of an inorganic Si-containing polymer component (PDMS) and organic PCL component were prepared. In this system, the PCL served as the switching segment and PDMS served as the soft segment to tailor mechanical properties. Networks were prepared by the rapid photochemical cure of AcO-PCL$_n$-*block*-PDMS$_{37}$-*block*-PCL$_n$-OAc macromers in which the PCL segment length was systematically tuned (n = 5, 10, 20, 30, 40 and 50). PCL segments of higher lengths (n = 30–50) underwent sufficient crystallization (24–30% crystallinity) and thus served as effective switching segments for resulting networks **(SMP1–3)**. As PCL segment length increased and hence crosslink density decreased, an unusual simultaneous increase of % e, E and TS was observed. **SMP1–3** exhibited excellent shape fixity and shape recovery.

Thus, inorganic–organic SMPs containing PDMS and PCL segments represent a new class of SMPs with desirable mechanical and shape memory properties.

Supplementary Material

Refer to Web version on PubMed Central for supplementary material.

Acknowledgements

We thank the Texas A&M University—Texas Engineering and Experiment Station (TEES) for financial support of the research. C.A.S. acknowledges an NSF Pre-doctoral Fellowship (NSF GK-12: DGE 0538547).

Notes and references

1. Lendlein A and Kelch S, Angew. Chem., Int. Ed, 2002, 41, 2034–2057.

2. Behl M and Lendlein A, Mater. Today (Oxford, UK), 2007, 10, 20–28.
3. Ratna D and Karger-Kocsis J, J. Mater. Sci, 2008, 43, 254–269.
4. Baer G, Wilson TS, Matthews DL and Maitland DJ, J. Appl. Polym. Sci, 2007, 103, 3882–3892.
5. Lendlein A and Kelch S, Clin. Hemorheol. Microcirc, 2005, 32, 105–116. [PubMed: 15764819]
6. Feninat FE, Laroche G, Fiset M and Mantovani D, Adv. Eng. Mater, 2002, 4, 91–104.
7. Neffe AT, Hanh BD, Steuer S and Lendlein A, Adv. Mater, 2009, 21, 1–5.
8. Judeinstein P and Sanchez C, J. Mater. Chem, 1996, 6, 511–525.
9. Hou Y, Matthews AR, Smitherman AM, Bulick AS,Hahn MS, Hou H, Han A and Grunlan MA, Biomaterials, 2008, 29, 3175–3184. [PubMed: 18455788]
10. Fichet O, Vidal F, Laskar J and Teyssie D, Polymer, 2005, 46, 37–47.
11. Park JH and Bae YH, Biomaterials, 2002, 23, 1797–1808. [PubMed: 11950050]
12. Stone DA and Allcock HR, Macromolecules, 2006, 39, 4935–4937.
13. Zhu G, Xu S, Wang J and Zhang L, Radiat. Phys. Chem, 2006, 75, 443–448.
14. Middleton JC and Tipton AJ, Biomaterials, 2000, 21, 2335–2346. [PubMed: 11055281]
15. Suggs LJ, Moore SA and Mikos AG, in Physical Properties of Polymers Handbook, ed. Mark JE, Springer, New York, NY, 2007, pp. 939–950.
16. Wang S, Lu L, Gruetzmacher JA, Currier BL and Yaszemski MJ, Biomaterials, 2006, 27, 832–841. [PubMed: 16102819]
17. Cao Q, Chen S, Hu J and Liu P, J. Appl. Polym. Sci, 2007, 106, 993–1000.
18. Zhuohong Y, Jinlian H, Yeqiu L and Lapyan Y, Mater. Chem. Phys, 2006, 98, 368–372.
19. Kim BK, Lee SY, Lee JS, Baek SH, Choi YJ, Lee JO and Xu M, Polymer, 1998, 39, 2803–2808.
20. Lu XL, Cai W and Gao ZY, J. Appl. Polym. Sci, 2008, 108, 1109–1115.
21. Lu XL, Sun ZJ, Cai W and Gao ZY, J. Mater. Sci. Mater. Med, 2008, 19, 395–399. [PubMed: 17607526]
22. Lu XL, Cai W, Zhiyong G and Tang WJ, Polym. Bull. (Berlin), 2007, 58, 381–391.
23. Wang W, Ping P, Chen X and Jing X, J. Appl. Polym. Sci, 2007, 104, 4182–4187.
24. Nagata M and Sato Y, J. Polym. Sci., Part A: Polym. Chem, 2005, 43, 2426–2439.
25. Min C, Cui W, Bei J and Wang S, Polym. Adv. Technol, 2005, 16, 608–615.
26. Nagata M and Kitazima I, Colloid Polym. Sci, 2006, 284, 380–386.
27. Lendlein A and Langer R, Science, 2002, 296, 1673–1676. [PubMed: 11976407]
28. Lendlein A, Schmidt A and Langer R, Proc. Natl. Acad. Sci.U. S. A, 2001, 98, 842–847. [PubMed: 11158558]
29. Curtis J and Colas A, in Biomaterials Science, ed. Ratner BD, Hoffman AS, Schoen FJ and Lemons JE, Elsevier Academic Press, San Diego, CA, 2004, pp. 697–707.
30. VanDyke ME, Clarson SJ and Arshady R, in Introduction to *Polymeric Biomaterials*, ed. Arshady R, Citus Books, London, 2003, pp. 109–135.
31. Porjazoska A, Cvetkovska M, Yilmaz OK, Baysal K,Apohan NK and Baysal BM, Glas. Hem. Tehnol. Maked, 2004, 23, 147–156.
32. Pitt CG, Chasalow FI, Hibionada YM, Klimas DM and Schindler A, J. Appl. Polym. Sci, 1981, 26, 3779–3787.
33. Wang Y, Ameer GA, Sheppard BJ and Langer R, Nat. Biotechnol, 2002, 20, 602–606. [PubMed: 12042865]
34. Nagata M and Sato Y, Polymer, 2004, 45, 87–93.
35. Fisher JP, Dean D, Engel PS and Mikos AG, Annu. Rev. Mater. Res, 2001, 31, 171–181.
36. Sperling LH, Introduction to Physical Polymer Science, John Wiley & Sons, Inc., New York, NY, 2001.
37. Lendlein A, Schmidt A, Schroeter M and Langer R, J. Polym. Sci., Part A: Polym. Chem, 2005, 43, 1369–1381.
38. Rabani G, Luftmann H and Kraft A, Polymer, 2006, 47, 4251–4260.

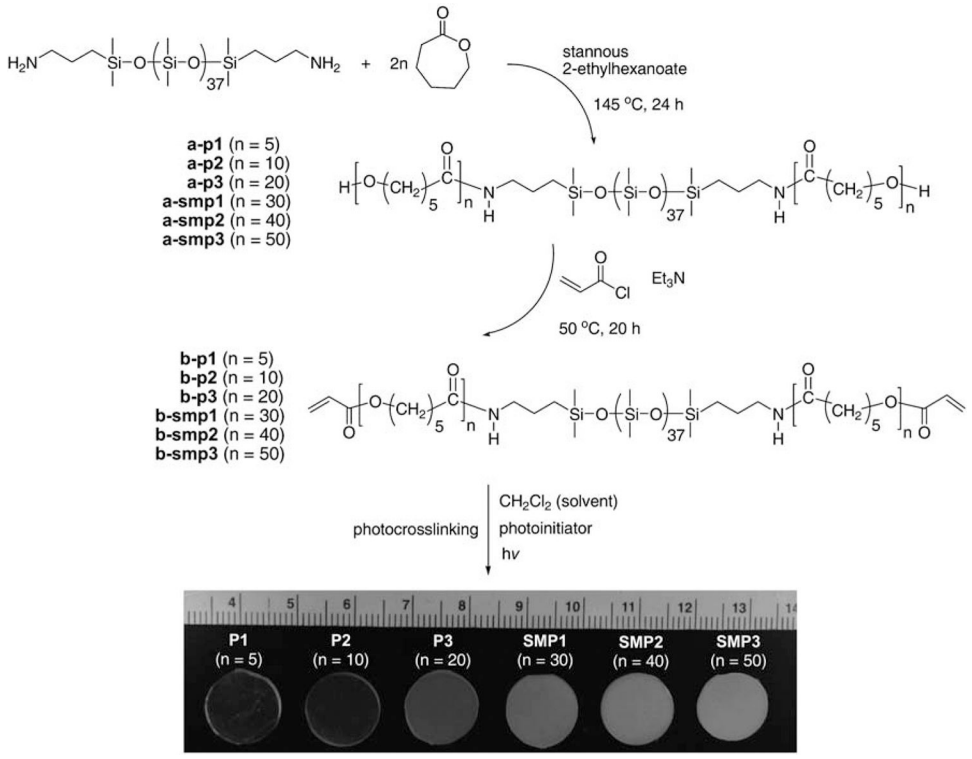

Fig. 1.

Synthesis and photochemical cure of AcO-PCL$_n$-*block*-PDMS$_{37}$-*block*-PCL$_n$-OAc (**b-p1–3** and **b-smp1–3**) to form **P1–3** and **SMP1–3** networks. **SMP1–3** exhibited shape memory behavior.

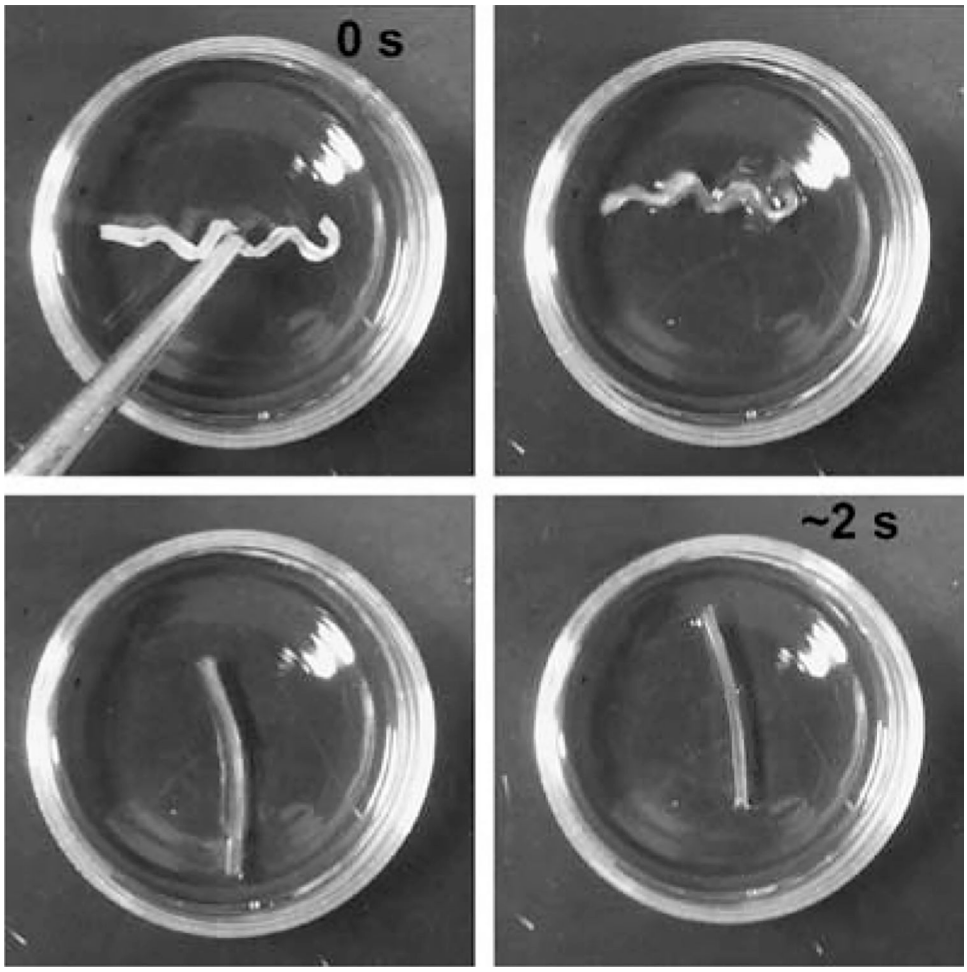

Fig. 2.

Time series photos showing shape memory effect of **SMP1** when placed in 60 °C DI water. The permanent shape is a flat, rectangular strip and the temporary shape is a spiral. The temporary shape was formed by sequentially elongating the specimen 150% at 60 °C, wrapping around a 3 mm diameter mandrel and fixing the shape by cooling to ~ 10 °C.

Table 1

Thermal and mechanical properties of networks[a]

Network	PCL (n)	M_n/g mol^{-1}	T_m/°C	ΔH_m/J g^{-1}	Cryst. (%)	Tensile modulus, E/MPa	Tensile strength, TS/MPa	Strain at break, ε (%)
P1	5	4324	—	—	0	0.7 ± 0.1	0.3 ± 0.1	156 ± 23
P2	10	5374	—	—	0	1.2 ± 0.1	0.4 ± 0.1	129 ± 11
P3	20	7654	34 ± 0.2	23 ± 2.0	17 ± 1.5	12.3 ± 0.5	2.8 ± 0.6	287 ± 11
SMP1	30	9934	52 ± 0.1	33 ± 1.9	24 ± 1.4	49.0 ± 0.8	7.0 ± 1.0	459 ± 61
SMP2	40	12 214	50 ± 0.1	37 ± 2.0	26 ± 1.4	47.4 ± 2.8	10.4 ± 0.3	814 ± 36
SMP3	50	14 494	51 ± 0.1	42 ± 0.5	30 ± 0.4	60.5 ± 0.7	15.9 ± 1.0	1197 ± 76

[a]PCL (thermoplastic, M_n = 50 400 g mol^{-1}): E (68 MPa), TS (14 MPa), % ε (830%).[34]All samples run in triplicate.

Table 2

Shape memory properties of networks[a]

Network	Cycle number (*N*)	R_r (*N*) (%)	$R_{r,tot}$ (*N*) (%)	R_f (*N*) (%)
SMP1	1	97.7 ± 0.7	97.7 ± 0.7	98.8 ± 0.3
	2	95.1 ± 2.9	93.0 ± 2.3	98.0 ± 0.5
	3	98.5 ± 0.7	91.5 ± 2.0	97.5 ± 0.3
	4	99.0 ± 0.3	90.6 ± 1.9	97.1 ± 0.4
	Ave (1–4)	*97.6 ± 1.1*	*93.2 ± 1.3*	*97.9 ± 0.4*
SMP2	1	94.2 ± 0.5	94.2 ± 0.5	98.9 ± 0.2
	2	97.2 ± 1.0	91.6 ± 1.4	99.1 ± 0.2
	3	98.6 ± 0.3	90.3 ± 1.6	99.1 ± 0.2
	4	98.7 ± 0.3	89.2 ± 1.8	99.1 ± 0.2
	Ave (1–4)	*97.2 ± 0.5*	*91.3 ± 1.3*	*99.1 ± 0.2*
SMP3	1	98.4 ± 1.4	98.4 ± 1.4	99.7 ± 0.2
	2	97.8 ± 0.2	96.2 ± 1.6	99.7 ± 0.2
	3	98.5 ± 0.3	94.8 ± 1.9	99.7 ± 0.2
	4	98.6 ± 0.3	93.4 ± 2.1	99.7 ± 0.2
	Ave (1–4)	*98.3 ± 0.6*	*95.7 ± 1.7*	*99.7 ± 0.2*

[a]All samples run in triplicate.